DESIGN AND TEST OF SELF-PROPELLED STRADDLE-TYPE *LYCIUM BARBARUM* L. SPRAYING MACHINE
/
自走式跨行枸杞喷药机设计与试验

Gao ZeNing[1)]; Chen QingYu[1)]; Hu GuangRui[1)]; Chen Chao[1)]; Li ChuanLin[1)]; Chen Jun*[1)]
[1)] College of Mechanical and Electronic Engineering, Northwest A&F University, Yangling 712100, China
Tel: +86 13572191773; E-mail: chenjun_jdxy@nwsuaf.edu.cn
DOI: https://doi.org/10.35633/inmateh-65-36

Keywords: Lycium barbarum *L, spraying, self-propelled straddle-type, phytosanitary liquid recovery, double-layer fence planting*

ABSTRACT
According to the planting agronomy of Lycium barbarum *L. in Ningxia, a self-propelled straddle-type sprayer was designed. The aim was to reduce the labour requirements, improve the spraying effect to the middle and lower parts of the canopy, reduce the influence of natural wind on droplet drift, and recycle excess phytosanitary liquid to reduce environmental pollution. Tests showed that the coverage rate of phytosanitary liquid on the leaf surface and back of the leaf peaked at 84.2% and 48.3%, respectively, when spraying pressure was high. Under different spraying distances, the coverage rate of phytosanitary liquid on leaf surface and back of leaf reached 73.3% and 38.3% at the shortest distance. The uniformity of the spray droplet distribution was good, the use error was less than 10%, and the excess liquid was effectively recovered.*

摘要
针对宁夏地区的双层篱架式枸杞种植农艺，设计了一种自走式跨行枸杞喷药机。目的在于减轻劳动强度，提高树冠中下部的喷药效果，减少自然风对液滴漂移的影响，并将多余药液进行回收以减少对环境的污染。试验结果表明：在不同的喷药压力下，叶面和叶背的药液覆盖率可达 84.2%和 48.3%；在不同的喷药距离下，叶面和叶背的药液覆盖率可达 73.3%和 38.3%。整机喷药的雾滴分布均匀性良好，施药量误差均在 10%以内，并且可以有效的对多余药液进行回收。

INTRODUCTION
Lycium barbarum L. is a deciduous shrub with infinite inflorescence, which is characteristic of *Lycium* in the Solanaceae family (*Chen et al., 2018; Zhao et al., 2021a, 2021b, 2021c, 2021d*). *L. barbarum* L. is mainly produced in Ningxia, Qinghai, Gansu, Tibet, and Inner Mongolia (*Chang, 2020; Li, 2021*). *L. barbarum* L. has both high medicinal value and high economic value (Li et al., 2017). In recent years, intelligent technologies have been widely used in planting, spraying and harvesting (*Hu et al., 2021*). Importantly, spraying of artificial phytosanitary liquid/chemicals to protect *L. barbarum* L. is still common practice in China, but this practice has many problems, including high labour costs, low efficiency, uneven spraying, and environmental pollution caused by excess chemicals (*Qi, 2017; Hu et al., 2021*).

In recent years, in order to improve the efficiency in spraying *L. barbarum* L., some large plantations have sprayed using unmanned aerial vehicles or orchard air-driven sprayers. Although the spraying efficiency is markedly improved by these methods, the effective utilization rate of phytosanitary liquid is very low. To address this, the Institute of Plant Protection, Ningxia Academy of Agriculture and Forestry Sciences designed a windproof spraying machine by covering the top and side of the spraying machine with a curtain. This reduced the influence of natural winds on droplet drift and improved the utilization rate of the phytosanitary liquid, but did not improve the spraying effect (*Zheng, 2015*). Following this, Ningxia University designed a windproof *L. barbarum* L. spraying machine in 2019 that reduced the influence of natural wind on droplets and used a three-dimensional spray rod configuration to even out the distribution of droplets deposited in the middle and lower parts of the canopy. Their sprayer also used pneumatic devices to provide kinetic energy for the droplets. However, these machines still do not consider the impact of excess phytosanitary liquid on the environment, and in the case of pneumatic devices, the droplets were less likely to attach to leaves and more likely to float into the air, which further increased the waste of phytosanitary liquid (*Hu, 2019*).

[1] *Zening Gao, M.S. Stud. Eng.; Qingyu Chen M.S. Stud. Eng.; Guangrui Hu M.S. Stud. Eng.; Chao Chen M.S. Stud. Eng.; Chuanlin Li M.S. Stud. Eng.; Jun Chen, Prof. Ph.D. Eng.*

In order to solve the above problems, this study designed a self-propelled straddle-type *L. barbarum* L. spraying machine to suit the double-layer hedgerow planting agronomy of *L. barbarum* L. utilized in Ningxia. This machine can effectively reduce the labour requirements, improve the spraying quality in the middle and lower parts of the canopy, reduce the influence of natural winds on droplet drift, and recycle excess phytosanitary liquid to reduce environmental pollution.

MATERIALS AND METHODS

Overall structure and working principle

The primary components of the machine include the windproof baffle, frame, phytosanitary liquid tank, wheels, universal wheels, stepping motor, phytosanitary liquid recovery baffle, phytosanitary liquid recovery tank, diaphragm pump, spraying distance adjusting device, pressure regulating valve, nozzle, spraying pipeline, and solenoid valve, as shown in Figure 1. The windproof baffles were fixed around the frame to form a relatively enclosed space. The phytosanitary liquid tank, diaphragm pump, pressure regulating valve, nozzle, injection pipeline, and solenoid valve constitute the injection system that sprays the liquid. The stepping motor, wheels, and universal wheels were installed under the frame to make the platform mobile.

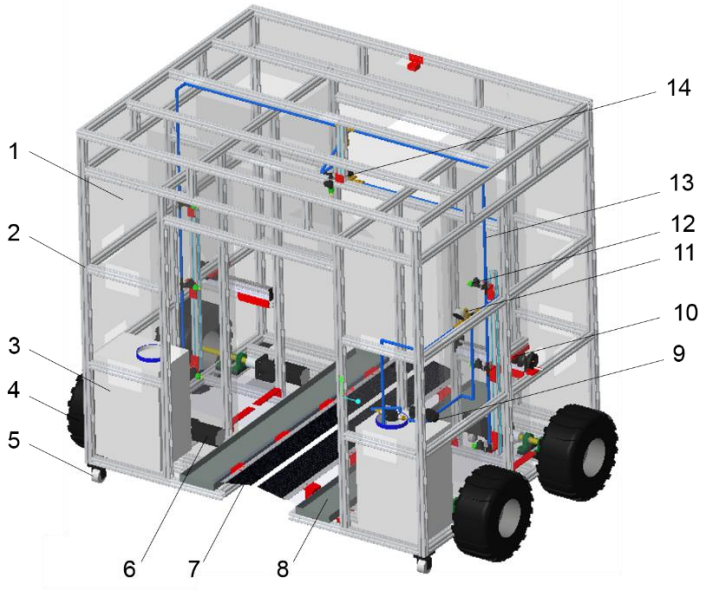

Fig. 1 - Schematic diagram of the machine

1) Windproof baffle; 2) frame; 3) phytosanitary liquid tank; 4) wheels; 5) universal wheel; 6) stepping motor; 7) phytosanitary liquid recovery baffle; 8) phytosanitary liquid recovery tank; 9) diaphragm pump; 10) spraying distance adjusting device; 11) pressure regulating valve; 12) nozzle; 13) spraying pipeline; 14) solenoid valve

During operation, the operator uses the controller to remotely direct the machines movements, either forward or backward over the crown of the *L. barbarum* L. plants. If there is any deviation in the traveling direction, the speed of wheels on both sides can be adjusted using the handle to realize differential steering. When spraying, the solenoid valve is kept open while the diaphragm pump provides the kinetic energy that drives droplets through the nozzle, which creates an even spray distribution, and the three-dimensional configuration of spraying rods effectively improves the spraying effectiveness for the middle and lower parts of the canopy. The windproof baffles surrounding the sprayer effectively reduce the influence of natural winds on the phytosanitary liquid drift and any droplets that do not attach to the blades will be collected and returned to the phytosanitary liquid recovery tank via the phytosanitary liquid recovery baffles. This significantly reduces the excess phytosanitary liquid allowed to enter and pollute the environment. In addition, the spraying pressure of the spraying machine can be adjusted using the pressure regulating valve, and the spraying distance can be specified by adjusting the nozzles on both sides to achieve the optimal spraying effect.

Design requirements and technical parameters

This study was conducted at the ecological *Lycium barbarum* L. science and technology demonstration base of the Zhengqihong *Lycium barbarum* L. Industry Development Co. Ltd. in Guyuan, Ningxia. The demonstration base utilizes the double-layer hedgerow planting mode, which is designed to encourage *L. barbarum* L. plants grow high and stably for a long time, improve fruit quality, reduce pests and diseases, and facilitate management (*Wu et al., 2016*). The *L. barbarum* L. variety used in the experiment was Keqi No. 2.

According to measurements, the planting agronomy of this variety was: row spacing of 3000 mm, plant spacing of 1100 mm, plant heights of 1320 mm~1640 mm, and canopy diameters of 750 mm~1200 mm. The machine was designed according to the planting agronomy and its main technical parameters are shown in Table 1.

Table 1

Main technical parameters of the spraying machine

Technical parameter	Value	Unit
Overall dimensions (length × width × height)	1600×2500×2000	mm
Overall weight	360	kg
Working speed	0.2~1.0	$m \cdot s^{-1}$
Track	2300	mm
Wheelbase	760	mm
Stepping motor torque	12.5	N·m
Reduction ratio	6	-
Maximum working height	1700	mm
Maximum working width	1000	mm
Ground clearance	120	mm

Key design components

Moving steering device and kinematic model

The moving steering device was mainly composed of the frame, tires, transmission shaft, bearing with seat, coupling, reducer, stepping motor, driver, single chip microcomputer, and remote controller, as shown in Figure 2. In order to simplify the steering mechanism, reduce the weight of the machine, and improve the field traversing performance, a "four-wheel drive and differential steering" driving mode was adopted for the moving steering device.

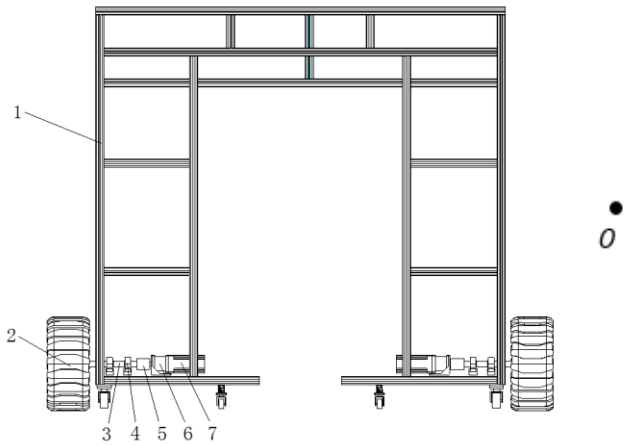

Fig. 2 - Schematic diagram of moving steering device

1) Frame; 2) tires; 3) transmission shaft; 4) bearing with seat; 5) coupling; 6) reducer; 7) stepping motor

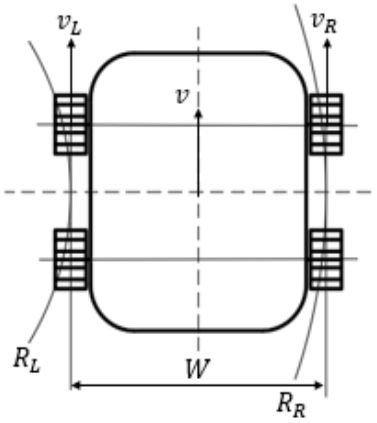

Fig. 3 - Kinematics model

Because the speeds of wheels on either side of the moving steering device were the same, the simplified two-wheel differential motion model could be used, as shown in Figure 3.

The linear speed is:

$$v_L = r \cdot u_L \quad (1)$$

$$v_R = r \cdot u_R \quad (2)$$

The angular velocity $\dot{\theta}$ of rotation around point *O* is:

$$\dot{\theta} = \frac{v_L}{R_L} = \frac{v_R}{R_R} \quad (3)$$

According to the relationship between R_R and R_L, R_L is:

$$\frac{v_L}{R_L} = \frac{v_R}{R_L + W} \tag{4}$$

$$R_L = \frac{v_L \cdot W}{v_R - v_L} \tag{5}$$

The angular velocity $\dot{\theta}$ can be obtained by bringing R_L into the equation as follows:

$$\dot{\theta} = \frac{v_R - v_L}{W} \tag{6}$$

The linear velocity *v* of the machine is:

$$v = \frac{v_R + v_L}{2} \tag{7}$$

The motion equation of the machine is:

$$\begin{cases} \dot{x} = v \cdot cos\theta \\ \dot{y} = v \cdot sin\theta \\ \dot{\theta} = \dfrac{v_R - v_L}{W} \end{cases} \tag{8}$$

The simplified model is:

$$q = \begin{bmatrix} \dot{\theta} \\ \dot{x} \\ \dot{y} \end{bmatrix} = \begin{bmatrix} -\dfrac{r}{w} & \dfrac{r}{w} \\ \dfrac{r}{2} cos\theta & \dfrac{r}{2} cos\theta \\ \dfrac{r}{2} sin\theta & \dfrac{r}{2} sin\theta \end{bmatrix} \begin{bmatrix} u_L \\ u_R \end{bmatrix} \tag{9}$$

where:

point *O* is the centre point of the turning radius; R_L is the turning radius of the left wheel, mm; R_R is the turning radius of the right wheel, mm; *r* is the wheel radius, mm; u_L is the angular velocity of the left wheel, rad/s; u_R is the angular velocity of the right wheel, rad/s; *v* is the linear speed of the machine, m/s; v_L is the linear speed of the left wheel, m/s; v_R is the linear speed of the right wheel, m/s; θ is the rotation angle of the machine, °; and W is the left and right wheel track, mm.

Control device

The control circuit diagram is shown in Figure 4. An Arduino single chip microcomputer was selected as the lower computer and a DC5V battery was used as the power supply. An 86 closed-loop stepping motor was selected as the driving motor and a ZDM-2HA860 driver powered by a DC72V battery was selected as the driver. A PS2 Bluetooth controller was used as the remote control. Two single-chip microcomputers communicate through TX and RX pins. The single-chip microcomputer *1* was connected to the Bluetooth receiving module to receive the remote control signals from the controller and, after signal processing, the control instructions are transmitted to the single-chip microcomputer *2*. The single-chip microcomputer *2* then controls the four stepping motors and uses different pulse frequencies to control the rotation speeds of the stepping motors. This process controls the vehicle speed and direction.

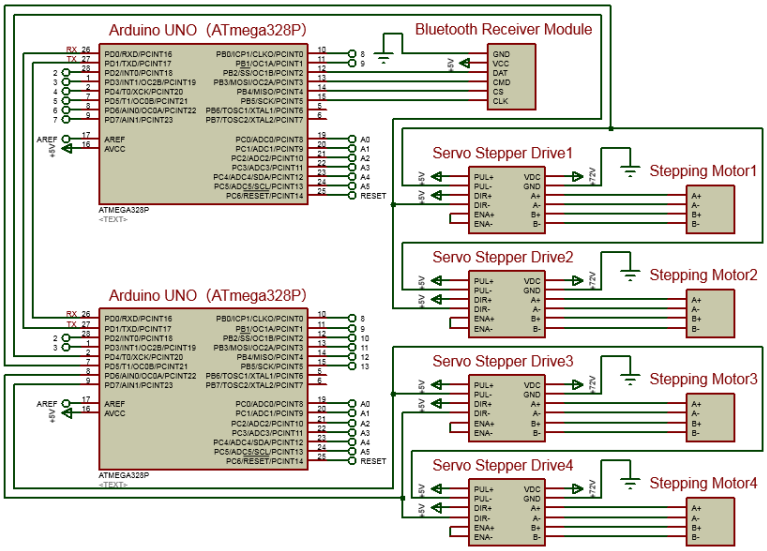

Fig. 4 - Control circuit diagram

Spray device

The schematic diagram of the spraying device is shown in Figure 5. It mainly consisted of the phytosanitary liquid tank, filter, diaphragm pump, check valve, nozzle, solenoid valve, pressure gauge, pressure regulating valve, and pressure relief valve, all of which were connected by pipelines and pipeline joints. After being pressurized by the diaphragm pump, the phytosanitary liquid flows out of the phytosanitary liquid tank and passes through the filter. The phytosanitary liquid then passes through the pressure regulating valve before reaching the solenoid valve. When the spraying operation starts, the solenoid valve opens and the phytosanitary liquid is sprayed from the nozzle at a constant pressure. A pressure gauge was installed at the outlet of the pressure regulating valve in the phytosanitary liquid pipeline to display the main pipeline pressure. When the pressure of the main pipeline is too high, the pressure relief valve relieves the pressure and any discharged phytosanitary liquid is returned back to the phytosanitary liquid tank, which is stirred.

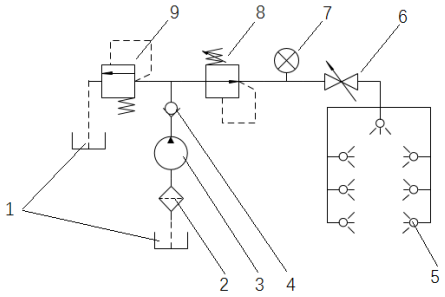

Fig. 5 - Schematic diagram of spraying device

1) Phytosanitary liquid tank; 2) filter; 3) diaphragm pump; 4) check valve; 5) nozzle; 6) solenoid valve; 7) pressure gauge; 8) pressure regulating valve; 9) pressure relief valve

In order to improve the uniformity of phytosanitary liquid coverage across the crown of the *L. barbarum* L. plants, a three-dimensional spray configuration was adopted wherein three nozzles were spaced evenly on each side. ARAG anti-drift nozzles, which were made in Italy and have a spray with a 110° sector shape (Qi, 2021), were used as shown in Figure 6. In order to ensure that the sprayed phytosanitary liquid covered the canopy of the *L. barbarum* L. plants, a minimum spraying distance was established according to the layout of the nozzles, calculated according to the following formula:

$$\frac{H}{6D} = tan\frac{\theta}{2} \tag{10}$$

$$D = \frac{H}{6tan\frac{\theta}{2}} \tag{11}$$

where: H is plant height, mm; D is the minimum spraying distance, mm; and θ is the included angle of spraying the fan-shaped surface, °.

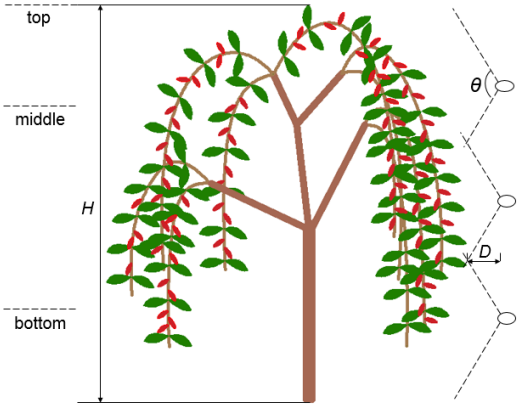

Fig. 6 - Schematic diagram of single side nozzle layout

The machine has a spraying position adjusting device which connects the three-dimensional spraying rods on each side with the modified GX80 sliding table, and the spraying distance can be adjusted within a range of 180 mm to 340 mm, as shown in Figure 1. The pressure adjusting valve was used so that the spraying pressure could be adjusted between 0.15 MPa and 0.35 MPa, as shown in Figure 1. The phytosanitary liquid recovery device which is positioned under the crown of *L. barbarum* L. when working, was designed to collect the phytosanitary liquid that did not attach to leaves, as shown in Figure 1.

Test conditions and design

From July 5th to 10th, 2021, a field experiment was conducted at the *L. barbarum* L. base of Zhengqihong Lycium barbarum L. Industry Development Co. Ltd., Yuanzhou District, Guyuan City, Ningxia, as shown in Figure 7. The test field was located at the coordinates 106.11 E and 36.29 N, and there was no rain or dew during the test. The temperature was 28~30°C, the wind speed was 1.6~2.0 m/s, and the spraying machine speed was 0.5 m/s.

Fig. 7 - Field trials

Nozzle test

The test instruments and materials included a stopwatch, measuring cup, electronic scale, and purified water. Each nozzle was labelled in turn and the spraying pressures were set to 0.15 MPa, 0.20 MPa, 0.25 MPa, 0.30 MPa, and 0.35 MPa in turn. The diaphragm pump was turned on and the liquid from each nozzle was collected with a measuring cup which was then put on the electronic scale for weighing after 1 min, this test process was repeated for three times (*Liu, 2019*).

Spraying effect test

Instruments and materials included water-sensitive test paper, purified water, and an electronic scale. A row of *L. barbarum* L. was randomly selected from the field and 10 evenly spaced *L. barbarum* L. trees within that row had 20 mm × 50 mm water-sensitive test papers fixed at their tops, middles (3/4 height), and bottoms (1/4 height) for observation, as shown in Figure 6.

Single factor experimental designs were used. First, at a spraying distance of 260 mm, spraying pressures of 0.15 MPa, 0.20 MPa, 0.25 MPa, 0.30 MPa and 0.35 MPa were tested. Next, the spraying pressure was fixed at 0.25 MPa and spraying was carried out at distances of 180 mm, 220 mm, 260 mm, 300 mm and 340 mm. Each of the above tests were repeated three times and the experimental water-sensitive test paper was taken back to the laboratory for quantification. The quantification indexes mainly included the coverage by phytosanitary liquid, the deposition density of droplets, and the uniformity of droplet distribution. The coverage of phytosanitary liquid was measured as the percentage of the total area covered with phytosanitary liquid. Droplet deposition density was calculated as the number of droplets per unit area. The degree of uniformity of droplet distribution was expressed by its coefficient of variation.

Application error and liquid recovery test

Test instruments and materials included a stopwatch, phytosanitary liquid tank, electronic scale, and purified water. Application error and liquid recovery were tested by operating the spraying machine for 1 min at spraying pressures of 0.15 MPa, 0.20 MPa, 0.25 MPa, 0.30 MPa and 0.35 MPa. The weight of the phytosanitary liquid tank before and after spraying and the weight of the liquid in the phytosanitary liquid recovery tank were recorded. Each test was repeated three times. Then the application error and recovery rates were calculated through the following formula:

$$U = \frac{q - q_0}{q_0} \times 100 \tag{12}$$

$$G = \frac{w}{q} \times 100 \tag{13}$$

where: U is the error rate of application rate, %; q is the actual dosage of phytosanitary liquid, L/min; q_0 is the predetermined dosage, L/min; G is the recovery rate of phytosanitary liquid, %; and w is the amount of recovered phytosanitary liquid, L/min.

RESULTS AND ANALYSIS

During the test, the spraying machine ran smoothly, the remote control device exhibited stable and reliable operation, the spray was uniform, and there were no out-of-control periods or rollover events during driving. At the same time, the spraying pressure and spraying distance was easily manually adjusted and consistent, and the overall performance was good. As a test prototype, initial observations showed that the spraying machine met the design requirements.

Nozzle test

The nozzle test results are shown in Table 2. The coefficient of variation was used as a measure of uniformity of nozzle spray. When the spraying pressure increases, the spray volume from the nozzle will also increase. The minimum variation coefficient was 0.331 and occurred when the spraying pressure was increased to 0.35 MPa, indicating that the uniformity of spray from each nozzle was the best at this pressure.

Table 2

Spray rate test results of nozzle

Nozzle number	Pressure (MPa)				
	0.15	0.20	0.25	0.30	0.35
1	277.79	316.51	341.28	361.79	378.41
2	284.89	323.57	352.29	373.06	382.39
3	260.16	297.50	321.33	342.51	358.04
4	259.23	296.69	319.98	343.47	361.53
5	258.38	295.74	318.55	338.95	369.99
6	285.74	325.74	347.40	372.26	388.88
7	284.61	328.69	350.07	370.81	388.11
Total spraying amount / ml	1910.79	2184.44	2350.90	2502.85	2627.35
Standard deviation / ml	13.10	14.89	15.26	15.39	12.41
Average value / ml	272.97	312.06	335.84	357.55	375.34
Coefficient of variation / %	0.0480	0.0477	0.0454	0.0430	0.0331

Spraying effect test

The spray test results under different spraying pressures are shown in Table 3. The droplet deposition density on the leaf surface and the back of the leaf peaked at 0.35 MPa, which indicated that with the increasing spray pressure the atomization effect was improved and droplet diameter decreased. The coverage rate of the phytosanitary liquid on the leaf surfaces peaked at 0.30 MPa, which indicated that when the spraying pressure is less than 0.30 MPa, the droplet particles had larger diameters and did not easily adhere to the leaves; but when the spraying pressure is greater than 0.30 MPa, the droplet particles have small diameters and droplet drift occurs, resulting in fewer droplets adhering to the leaves. The coefficients of variation of both the fronts and backs of the leaves were about 1%, which showed good uniformity of droplet distribution.

Table 3

Test results of spraying effect under different spraying pressure

Pressure (MPa)	Leaf	Canopy	Droplet coverage rate (%)		Droplet deposition density (pcs/cm^2)		Uniformity of droplet distribution (%)	
0.15	front	top	72.5	65	16	18	0.84	0.94
		middle		77.5		14		1.00
		bottom		75		16		0.59
	back	top	42.5	35	9	10	0.86	0.71
		middle		47.5		8		0.92
		bottom		45		8		0.94

Table 3
(continuation)

Pressure (MPa)	Leaf	Canopy	Droplet coverage rate (%)		Droplet deposition density (pcs/cm²)		Uniformity of droplet distribution (%)	
0.20	front	top	75.8	60	18	20	0.27	0.86
		middle		82.5		17		1.51
		bottom		85		18		0.96
	back	top	42.5	42.5	9	12	1.03	0.81
		middle		42.5		8		1.23
		bottom		42.5		7		1.06
0.25	front	top	80.0	70	18	19	1.26	0.99
		middle		85		17		1.10
		bottom		85		19		1.68
	back	top	46.7	42.5	8	9	1.27	1.13
		middle		52.5		7		1.18
		bottom		45		8		1.49
0.30	front	top	84.2	80	19	19	1.09	1.09
		middle		87.5		17		0.96
		bottom		85		20		1.24
	back	top	48.3	45	9	11	1.00	1.11
		middle		50		7		1.03
		bottom		50		8		0.87
0.35	front	top	77.5	70	21	23	1.00	1.14
		middle		85		19		0.86
		bottom		77.5		21		1.01
	back	top	47.5	45	10	12	0.73	0.80
		middle		50		8		0.74
		bottom		47.5		11		0.65

The test results at different spraying distances are shown in Table 4. The droplet deposition density on the leaf surface and back of the leaf was highest when the distance was shortest, 180 mm. This indicated that, with increasing spraying distance, fewer droplets attach to the leaves due to insufficient kinetic energy. The coverage rate of the phytosanitary liquid on the leaf surface and back of the leaf peaked at 340 mm, but the deposition density of droplets was the lowest at this distance, indicating that at large distances the spray overlap will allow small droplets to converge into larger droplets and attach to the leaves, thus improving the coverage of phytosanitary liquid. The coefficients of variation of both the fronts and backs of leaves were about 1%, which showed good uniformity of droplet distribution.

Table 4

Test results of spraying effect under different spraying distance

Distance (mm)	Leaf	Canopy	Droplet coverage rate (%)		Droplet deposition density (pcs/cm²)		Uniformity of droplet distribution (%)	
180	front	top	70.0	65.0	27	28	1.46	1.33
		middle		67.5		27		1.75
		bottom		77.5		27		1.31
	back	top	34.2	35.0	12	15	1.22	1.50
		middle		35.0		12		1.10
		bottom		32.5		9		1.07

Table 4
(continuation)

Distance (mm)	Leaf	Canopy	Droplet coverage rate (%)		Droplet deposition density (pcs/cm²)		Uniformity of droplet distribution (%)	
220	front	top	66.7	55.0	25	24	1.00	0.76
		middle		70.0		28		1.50
		bottom		75.0		22		0.75
	back	top	30.8	25.0	12	14	1.07	1.63
		middle		37.5		14		0.86
		bottom		30.0		9		0.71
260	front	top	65.0	57.5	25	24	1.24	1.17
		middle		67.5		26		1.23
		bottom		70.0		26		1.31
	back	top	30.8	30.0	11	12	0.95	1.03
		middle		32.5		11		0.84
		bottom		30.0		9		0.98
300	front	top	68.3	57.5	23	24	1.08	1.16
		middle		75.0		22		1.10
		bottom		72.5		24		0.99
	back	top	31.7	32.5	12	13	1.05	0.79
		middle		35.0		12		1.46
		bottom		27.5		12		0.88
340	front	top	73.3	62.5	19	20	1.10	1.61
		middle		77.5		18		1.00
		bottom		80.0		18		0.71
	back	top	38.3	35.0	10	12	1.05	1.29
		middle		37.5		10		0.98
		bottom		42.5		8		0.90

Application error and liquid recovery test

The error in the application amount and the phytosanitary liquid recovery test are shown in Table 5. When working in the field, the error in the application amount under different spraying pressures remained within 10% and the phytosanitary liquid recovery device was able to collect the droplets that did not attach to the leaves. From the test results of the phytosanitary liquid recovery rate, it was also found that with increasing of spraying pressure, the phytosanitary liquid recovery rate gradually decreased. This indicated that more droplets had attached to the leaves and the phytosanitary liquid utilization rate was improved.

Table 5

Application error and liquid recovery test results

Pressure /MPa	Scheduled dosage /（L/min）	Average dosage /（L/min）	Error rate /%	Average recovery /（L/min）	rate of recovery /%
0.15	1.911	1.775	7.12	0.867	48.85
0.20	2.184	2.047	6.27	0.807	39.43
0.25	2.351	2.557	8.76	1.035	40.48
0.30	2.503	2.740	9.47	1.027	37.47
0.35	2.627	2.706	3.01	0.974	36.00

CONCLUSIONS

Considering the specific requirements of the double-layer hedgerow planting mode of *Lycium barbarum* L., a self-propelled straddle-type phytosanitary liquid spraying machine was designed, the key components and parameters of the machine were determined, and a prototype was made. The machine adopted the "four-wheel drive and differential steering" driving mode, which is a simple steering mechanism that reduces machine weight and has good field traversal performance and operability. The three-dimensional spraying configuration with spray rods on both sides effectively improved the spraying of the middle and lower portions of the *L. barbarum* L. and made the spraying more uniform over the entire plant. The phytosanitary liquid recovery device effectively recovered most of the phytosanitary liquid that was not attached to the leaves and reduced the pollution to the environment.

ACKNOWLEDGEMENT

The authors would like to acknowledge Zhengqihong *Lycium barbarum* L. Industry Development Co. Ltd. for their support during field testing.

REFERENCES

[1] Chang, X. M. (2020). Pollution-free cultivation of *Lycium barbarum* L.. *Agricultural Technology and Equipment*, (03), 149-150.

[2] Chen, J., Zhao, J., Chen, Y., Bu, L. X., Hu, G. R., & Zhang, E. Y. (2019). Design and experiment on vibrating and comb brushing harvester for *Lycium barbarum* L.. *Transactions of the Chinese Society of Agricultural Machinery*, 50(01), 152-161+95.

[3] Hu, G. R., Kong, W. Y., Qi, C., Zhang, S., Bu, L. X., Zhou, J. G., & Chen, J. (2021). Optimization of the navigation path for a mobile harvesting robot in orchard environment. *Transactions of the Chinese Society of Agricultural Engineering*, 37(09), 175-184.

[4] Hu, X. D. (2019). *Design and research of windproof plant protection machine*. [Master dissertation, Ningxia University]. CNKI.

[5] Hu, X. D., Zhang, D. F., He, J., Hu, C. & Bai, F. (2021). Development and test of wind-proof wolfberry plant protection machine. *Journal of Agricultural Mechanization Research*, 43(01), 119-124+145.

[6] Li, J. H. (2017). *Design of directional air-blowing wolfberry sprayer*. [Master dissertation, Ningxia University]. CNKI.

[7] Li, X. P. (2021). Study on utilization value and cultivation technology of *Lycium barbarum* L.. *Seed Science and Technology*, 39(05), 24-25.

[8] Liu, L. M., Zhang, X. H., Shi, G. Z., Jiang, H. H., Bai, P., & Li, J. (2019). Design and test of polymorphic automatic target air-blast spray test-bed. *Jiangsu Agricultural Sciences*, 47(13), 260-263.

[9] Qi, C. (2021). *Variable spraying control system for sprayer*. [Master dissertation, Northwest A&F University]. CNKI.

[10] Qi, P. (2017). Introduction of common plant protection machinery. *Scientific Farming*, (08), 61-62.

[11] Wu, Z. S., Ma, M. C., & Ma, M. R. (2016). Management techniques of trellis cultivation for organic *Lycium barbarum* L. in Qaidam area of Qinghai province. *Protection Forest Science and Technology*, (08), 16-18+33.

[12] Zhao, J., & Chen, J. (2021). Detecting maturity in fresh *Lycium barbarum* L. fruit using colour information. *Horticulturae*, 7(5).

[13] Zhao, J., Ma, T., Inagaki, T., Chen, Q. Y., Gao, Z. N., Sun, L. J., Cai, H. X., Chen, C., Li, C. L., Zhang, S. X., Tsuchikawa, S., & Chen, J. (2021). Finite element method simulations and experiments of detachments of *Lycium barbarum* L. *Forests*, 12(6).

[14] Zhao, J., Ma, T., Inagaki, T., Chen, Y., Hu, G. R., Wang, Z. W., Chen, Q. Y., Gao, Z. N., Zhou, J. G., Wang, M. H., Tsuchikawa, S., & Chen, J. (2021). Parameter optimization of vibrating and comb-brushing harvesting of Lycium barbarum L. based on FEM and RSM. Horticulturae, 7(9).

[15] Zhao, J., Tsuchikawa, S., Ma, T., Hu, G. R., Chen, Y., Wang, Z. W., Chen, Q. Y., Gao, Z. N., & Chen, J. (2021). Modal analysis and experiment of a *Lycium barbarum* L. shrub for efficient vibration harvesting of fruit. *Agriculture-Basel*, 11(6).

[16] Zheng, Q. W. (2015). Ningxia academy of agriculture and forestry sciences has achieved remarkable results in the transformation of windproof machinery for *Lycium barbarum* L. disease and insect control. *Pesticide Market News*, (25), 51.